Parathyroid Scintigraphy in Patients with Primary Hyperparathyroidism: ^{99m}Tc Sestamibi SPECT and SPECT/CT[1]

TEACHING POINTS
See last page

CME FEATURE
See accompanying test at http://www.rsna.org/education/rg_cme.html

LEARNING OBJECTIVES FOR TEST 5

After reading this article and taking the test, the reader will be able to:

- Explain the physiologic principles underlying ^{99m}Tc parathyroid scintigraphy.
- Describe the various methods used for ^{99m}Tc parathyroid scintigraphy, with emphasis on SPECT and SPECT/CT.
- Define the criteria for identifying and localizing parathyroid adenomas on SPECT and SPECT/CT images.

Hedieh K. Eslamy, MD • Harvey A. Ziessman, MD

The clinical diagnosis of primary hyperparathyroidism is based largely on serum laboratory test results, as patients often are asymptomatic. Surgery, often with bilateral exploration of the neck, has been considered the definitive treatment for symptomatic disease. However, given that approximately 90% of cases are due to a single parathyroid adenoma, a better treatment may be the selective surgical excision of the hyperfunctioning parathyroid gland after its preoperative identification and localization at radiologic imaging. Scintigraphy and ultrasonography are the imaging modalities most often used for preoperative localization. Various scintigraphic protocols may be used in the clinical setting: Single-phase dual-isotope subtraction imaging, dual-phase single-isotope imaging, or a combination of the two may be used to obtain planar or tomographic views. Single photon emission computed tomography (SPECT) with the use of technetium-99m (^{99m}Tc) sestamibi as the radiotracer, especially when combined with x-ray–based computed tomography (CT), is particularly helpful for preoperative localization: The three-dimensional functional information from SPECT is fused with the anatomic information obtained from CT. In addition, knowledge of the anatomy and embryologic development of the parathyroid glands and the pathophysiology of primary hyperparathyroidism aid in the identification and localization of hyperfunctioning glands.

Abbreviations: MIP = maximum intensity projection, PTH = parathyroid hormone

RadioGraphics 2008; 28:1461–1476 • **Published online** 10.1148/rg.285075055 • **Content Codes:** CT HN NM

[1]From the Division of Nuclear Medicine, the Russell H. Morgan Department of Radiology, Johns Hopkins Medical Institutions, 601 N Caroline St, Suite 3231, Baltimore, MD 21278. Presented as an education exhibit at the 2006 RSNA Annual Meeting. Received March 26, 2007; revision requested July 25; final revision received February 15, 2008, and accepted February 20. All authors have no financial relationships to disclose. **Address correspondence to** H.A.Z. (e-mail: *hziessm1@jhmi.edu*).

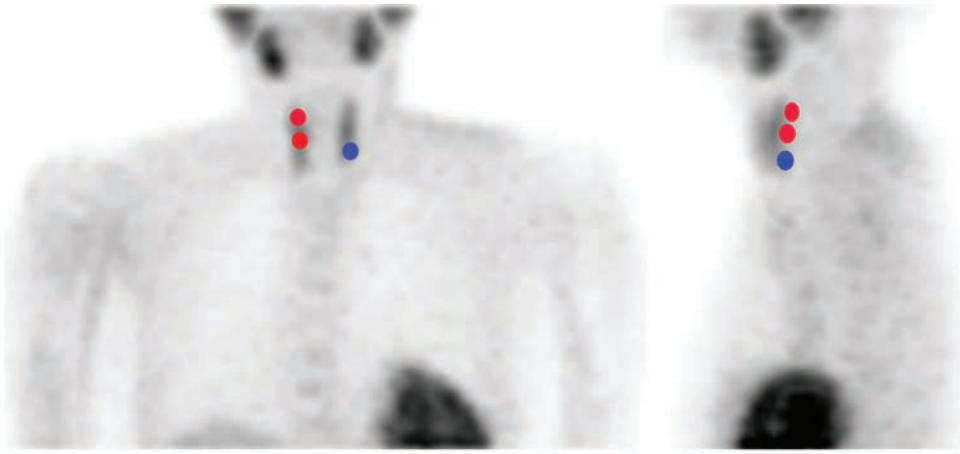

a. b.

Figure 1. MIP images from SPECT show the locations of eutopic parathyroid glands in anterior **(a)** and lateral **(b)** views. Eutopic superior parathyroid glands (red dots) are situated posterior to the superior and middle third of the thyroid lobe. Eutopic inferior parathyroid glands (blue dot) are posterior, lateral, or anterior to the inferior third of the thyroid lobe.

Introduction

Primary hyperparathyroidism is the most common cause of hypercalcemia in otherwise healthy outpatients. Classic manifestations of primary hyperparathyroidism, such as nephrocalcinosis, nephrolithiasis, and osteitis fibrosa cystica, are rarely seen today. Most people affected by the disorder are asymptomatic, with elevated calcium levels that are detected at routine blood sampling (1,2). In up to 90 percent of patients with primary hyperparathyroidism, the underlying cause is a solitary adenoma (3). Historically, bilateral cervical exploration for localization of all four parathyroid glands and removal of any that are grossly enlarged has been the standard surgical treatment for hyperparathyroidism. However, because most patients have single-gland disease, bilateral neck exploration in all patients with hyperparathyroidism is not routinely necessary. To minimize the duration of surgery and the risk of complications, a focused approach with unilateral cervical exploration and removal of the presurgically identified adenoma is preferable (4). Minimally invasive and endoscopic parathyroidectomies with intraoperative assays of parathyroid hormone (PTH) levels represent further refinements of the therapeutic approach (5). Preoperative technetium-99m (^{99m}Tc) sestamibi scintigraphy is widely used to localize adenomas. The advantage of using ^{99m}Tc sestamibi single photon emission computed tomography (SPECT) in combination with x-ray–based computed tomography (CT) is that it allows localization of parathyroid adenomas in three dimensions.

Anatomy of the Parathyroid and Thyroid Glands

The parathyroids are small lentiform glands that generally are located adjacent to the thyroid gland. Normal parathyroid glands measure approximately 6 mm in length, 3–4 mm in transverse diameter, and 1–2 mm in anteroposterior diameter (6). The parathyroid glands weigh 29.5 mg ± 17.8 (mean ± standard deviation), with a reported upper limit of 65 mg (7).

Most people have two superior and two inferior parathyroid glands; however, there may be only three, or one or more supernumerary glands may be present. Normally, parathyroid glands are located within the visceral space of the neck, posterior to the thyroid gland, in the vicinity of the tracheoesophageal groove. They may be located either inside or outside the thyroid capsule (intra- or extracapsular), but they most commonly appear in the latter location. Other structures in the vicinity of the tracheoesophageal groove are the

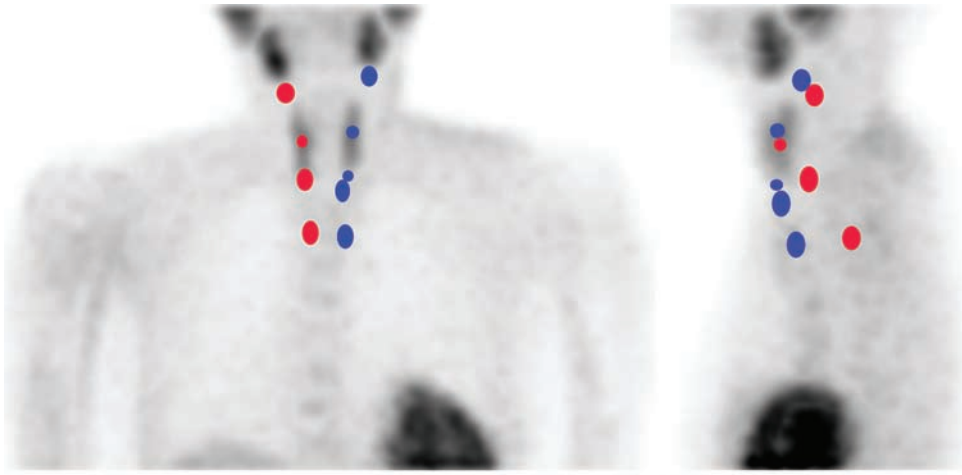

a. b.

Figure 2. MIP images from SPECT show the locations of ectopic parathyroid glands in anterior **(a)** and lateral **(b)** views. Ectopic superior glands (red dots, from top to bottom) may be in the carotid sheath; intrathyroidal; in the tracheoesophageal groove, retroesophageal, or paraesophageal; or posterosuperior mediastinal. Ectopic inferior glands (blue dots, from top to bottom) may be submandibular, intrathyroidal, in the thyrothymic ligament, intrathymic (in the neck), or anterosuperior mediastinal; except in intrathyroidal locations, their positions are anterior to those of superior glands.

paratracheal lymph node chain and the recurrent laryngeal nerve (6).

The inferior and superior parathyroid glands are paired structures that arise from the third and fourth branchial pouches, respectively. The superior parathyroid glands and lateral anlagen of the thyroid gland arise from the fourth branchial pouch. Being closely related to the thyroid gland, they normally undergo a minimal descent; therefore, their positions are relatively constant. The inferior parathyroid glands and thymus arise from the third branchial pouch. The inferior parathyroid glands, along with the thymic anlage, descend a greater distance and therefore have more variable positions (8).

Teaching Point

Eutopic superior parathyroid glands are posterior to the superior or middle third of the thyroid lobe; eutopic inferior parathyroid glands are anterior, lateral, or posterior to the inferior third of the thyroid lobe (Fig 1) (9). The inferior parathyroid glands are typically located anterior to, and the superior glands, posterior to, the juxtaposition of the inferior thyroid artery and recurrent laryngeal nerve (8). Superior and inferior parathyroid glands that are located above or below the level of the thyroid gland in the neck or mediastinum or posterior to the pharynx or esophagus are considered ectopic (Fig 2). Superior parathyroid glands at the level of the inferior third of the thyroid lobe, in the tracheoesophageal groove, also are considered ectopic (9).

Eutopic superior parathyroid glands are located on the posterior aspect of the superior or middle third of the thyroid lobe in more than 90% of the general population. The location of an ectopic superior parathyroid gland may be above the upper pole of the thyroid lobe (<1%); posterior to the pharynx or esophagus, in either the neck or the superior mediastinum (1%–4%); or intrathyroidal (<3%). Eutopic inferior parathyroid glands are located at the level of the inferior pole of the thyroid lobe, in its posterior, lateral, or anterior aspects (61%). Ectopic inferior parathyroid glands may be located in the neck, inferior to the lower pole of the thyroid lobe, either in the thyrothymic ligament or associated with the cervical portion of the thymus (26%); on or adjacent to the posterior aspect of the middle third of the thyroid lobe (7%); in the anterior mediastinum (4%–5%); intrathyroidal (<3%); or along the carotid sheath (<1%–2%). In the anterior mediastinum, inferior parathyroid glands may be situated within the thymus, at the posterior aspect of the thymic capsule, or in contact with the great vessels of the mediastinum (8).

Parathyroid glands are composed of chief cells, oxyphil cells, and transitional oxyphil cells mixed with adipose tissue. Chief cells secrete parathyroid hormone. The oxyphil cells are packed with mitochondria, and their function is unknown (10).

Primary Hyperparathyroidism

In the United States, the prevalence of primary hyperparathyroidism in women is two to three per 1000 in the general population, and that in men is approximately one per 1000. Laboratory findings in patients with primary hyperparathyroidism include persistent hypercalcemia and excessive serum parathyroid hormone (PTH) levels. Malignancy, the second most common cause of hypercalcemia, is distinguished from primary hyperparathyroidism by low or suppressed parathyroid hormone levels. Surgery is the definitive treatment for patients with symptomatic primary hyperparathyroidism (1,2).

Primary hyperparathyroidism may be asymptomatic (75%–80% of cases) or symptomatic (20%–25% of cases) (11). Symptomatic disease has no specific clinical manifestations, but nonspecific symptoms such as weakness, mild depression, fatigue, and anorexia may occur (1). The signs and symptoms of hyperparathyroidism largely represent hypercalcemia, which may affect multiple systems (neurologic, cardiovascular, gastrointestinal, renal, or musculoskeletal) (1,2).

Teaching Point

Primary hyperparathyroidism may be sporadic or familial. The cause in most cases is a single parathyroid adenoma (90% of cases); less common causes include double adenomas (4%), hyperplasia of multiple glands (6%), and parathyroid carcinoma (<1%) (3). Hereditary disorders, including familial hyperparathyroidism, multiple endocrine neoplasia syndrome (types 1 and 2A), and hyperparathyroidism–jaw tumor syndrome, account for up to 10% of cases of primary hyperparathyroidism and often involve multiple-gland hyperplasia rather than a single parathyroid adenoma. Benign familial hypocalciuric hypercalcemia is an autosomal dominant disorder characterized by hypercalcemia and relative hypocalciuria. It may be distinguished from primary hyperparathyroidism by the presence of a calcium-creatinine clearance ratio of less than 0.01 (1).

Patients with a normal serum calcium level and an elevated PTH level most likely have mild secondary hyperparathyroidism due to insufficient levels of vitamin D, calcium, or both. End-stage renal disease is the most common cause. In patients with renal failure, PTH secretion is stimulated by hypocalcemia (which results from low concentrations of 1,25-dihydroxy-vitamin D caused by decreased renal production) and hyperphosphatemia. Prolonged hypocalcemia and hyperphosphatemia may evolve into a state of autonomous PTH secretion and hypercalcemia referred to as tertiary hyperparathyroidism (1). A National Institutes of Health consensus panel on primary hyperparathyroidism revised parathyroid surgery guidelines for asymptomatic patients in 2002. Surgery is indicated if one or more of the following factors are present: a serum calcium level 1.0 mg/dL above the upper limit of the normal range; a 24-hour urinary calcium level of more than 400 mg; creatinine clearance reduced by 30%; a bone mineral density T-score of less than –2.5 SD measured at any site; age of less than 50 years; and undesirability or impossibility of medical surveillance. The panel confirmed the recommendation of parathyroidectomy for any patient with symptomatic hyperparathyroidism involving target organs, such as patients with nephrolithiasis, severe bone disease, or neuromuscular dysfunction (12).

Surgical Treatment

Definitive treatment of primary hyperparathyroidism involves the surgical excision of hyperfunctioning parathyroid glands. In the past, this was achieved with bilateral neck exploration and removal of the enlarged gland or glands. Improved presurgical imaging localization, intraoperative PTH assays, and hand-held gamma detectors have made the selective excision of preoperatively identified hyperfunctioning parathyroid glands possible. The most recently developed surgical approach involves the creation of a small unilateral incision to allow the insertion of surgical instruments, either alone (minimally invasive parathyroidectomy) or with a videoscope (endoscopic parathyroidectomy) (5,8,13). During surgery, blood is drawn for PTH assays before (baseline) and after the excision of a hyperfunc-

tioning gland. A decrease of more than 50% from the baseline PTH value at 5–10 minutes after resection is suggestive of a single site of primary hyperparathyroidism (generally, a single parathyroid adenoma). If such a drop does not occur, either double parathyroid gland adenomas or four-gland hyperplasia is likely, and the patient usually must undergo bilateral neck exploration (5). For minimally invasive surgery, precise preoperative localization is critical.

Variation in parathyroid gland locations is due not only to the glands' variable embryologic descent but also to the tendency of enlarged superior parathyroid glands to migrate posteriorly and inferiorly through fibroareolar tissue, which offers little resistance (8,9). In a series of 231 patients who underwent surgical treatment for hyperparathyroidism, 37 (16%) had ectopic parathyroid glands. Twenty-three had inferior glands in an intrathymic (30%), anterosuperior mediastinal (22%), or intrathyroidal (22%) site; within the thyrothymic ligament (17%); or in a submandibular location (9%). Fourteen had ectopic superior parathyroid glands in the tracheoesophageal groove (43%); in a retroesophageal (22%), posterosuperior mediastinal (14%), or intrathyroidal (7%) site; within the carotid sheath (7%); or in a paraesophageal location (7%) (9).

Surgical excision of an ectopic superior parathyroid gland located at the level of the inferior thyroid gland in the tracheoesophageal groove is often difficult because of the close proximity of the gland to the recurrent laryngeal nerve. Preoperative knowledge of the likelihood of an ectopic superior gland in the tracheoesophageal groove facilitates surgical exploration, and the surgeon may choose a lateral approach to improve visualization of the lateral laryngeal nerve and decrease the risk of inadvertent nerve injury. Thus, localization of a parathyroid adenoma in three dimensions and differentiation of a superior parathyroid gland at the level of the inferior thyroid from an inferior parathyroid gland is desirable (14,15). A superior gland is located posterior to an inferior gland. SPECT, particularly when combined with CT, often makes this distinction possible preoperatively.

Optimal Preoperative Imaging

Comparisons of different parathyroid imaging methods have shown the superiority of scintigraphy for preoperative localization. One recent meta-analysis of the medical literature reported that the overall sensitivity of dual-phase ^{99m}Tc sestamibi scintigraphy in comparison with high-resolution ultrasonography (US) was 88% versus 78% for single adenomas, 30% versus 16% for double adenomas, and 44% versus 35% for multiple-gland hyperplasia (3).

Neck US may be helpful for correlating or confirming uncertain findings and occasionally may be diagnostic in patients with a negative result at ^{99m}Tc sestamibi scintigraphy. Combined US and ^{99m}Tc sestamibi scintigraphy are reported to have increased sensitivity for the preoperative localization of parathyroid adenomas (16,17). However, both techniques remain similarly insensitive for the detection of multiglandular disease and double adenomas. Neck US yields suboptimal results in patients with multinodular thyroid disease, a short or thick neck, or an adenoma in a "silent" area such as the mediastinum, tracheoesophageal groove, or retroesophageal region (18).

Contrast material–enhanced CT and magnetic resonance (MR) imaging also may be effective for localizing parathyroid adenomas; however, they are used less commonly for preoperative localization than for the detection of a suspected ectopic mediastinal parathyroid adenoma in the setting of failed parathyroidectomy (19). Thin-section contrast-enhanced CT is reported to have a sensitivity ranging from 46% to 87% for the detection of parathyroid adenomas (20). The reported sensitivity of MR imaging for detection of parathyroid adenomas ranges from 65% to 80%, and the modality is not widely used for preoperative localization (20).

Parathyroid Scintigraphy

The first radionuclide imaging technique widely used in the 1980s for hyperfunctioning parathyroid localization was thallium-201 (^{201}Tl) scintigraphy. Since ^{201}Tl is taken up by both the thyroid and parathyroid, it was used in conjunction with ^{99m}Tc pertechnetate, which is taken up only by the thyroid. The ^{99m}Tc scintigram then was digitally subtracted from the ^{201}Tl scintigram to allow parathyroid localization (20). In 1989, Coakley and colleagues reported the use of ^{99m}Tc sestamibi for parathyroid scintigraphy (21). The new radionuclide rapidly replaced ^{201}Tl because

of superior image quality, more favorable dosimetry, and improved detection sensitivity with its use (22). A variation of this method is the subtraction of thyroid images obtained with iodine-123 (^{123}I) or ^{99m}Tc pertechnetate from those obtained with ^{99m}Tc sestamibi (23,24). Taillefer et al recommended the use of a single-isotope dual-phase (early- and delayed-phase) scintigraphic technique, a suggestion based on their observation that ^{99m}Tc sestamibi washes out more rapidly from the thyroid gland than from hyperfunctioning parathyroid glands (25). Another myocardial perfusion agent, ^{99m}Tc tetrofosmin, also has been used for parathyroid scintigraphy, but the experiential data for this method are more limited.

^{99m}Tc sestamibi consists of lipophilic cationic molecules. After intravenous injection, the molecules are distributed according to blood flow in the body, cross the cell membranes by passive diffusion, and become concentrated intracellularly in the region of the mitochondria (26). The detectability of parathyroid adenomas and hyperplastic parathyroid glands is related to the presence of mitochrondria-rich oxyphil cells. Although first used as a cardiac imaging agent, this radiopharmaceutical also was found to have increased uptake in a variety of benign and malignant tumors.

^{99m}Tc sestamibi normally is distributed to the parotid and submandibular salivary glands, thyroid gland, heart, and liver; uptake is not seen in normal parathyroid glands (Fig 3). Retention of the radiotracer is commonly seen in the arm vein through which the infusion was administered. Mild to moderate radiotracer accumulation in the oral cavity may occur, secondary to radiotracer secretion from the salivary glands. There is variable mild generalized uptake in the bone marrow. In younger individuals, mild to moderate thymic uptake may be seen. Uptake also may be seen in brown fat (typically in a supraclavicular location) (Fig 4b).

Teaching Point

Three general techniques of radionuclide scintigraphy are commonly used for the detection and visualization of hyperfunctioning parathyroid glands: single-phase dual-isotope subtraction imaging, dual-phase single-isotope imaging, and a combination of the two (27).

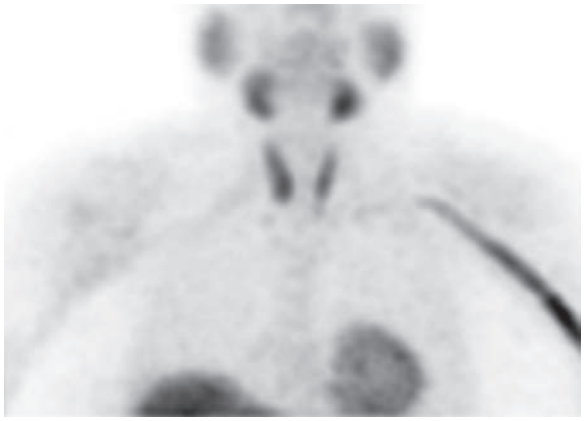

Figure 3. Anterior MIP image from SPECT shows normal early-phase distribution of ^{99m}Tc sestamibi, with the most intense uptake in the parotid and submandibular glands, thyroid gland, heart, and liver. The thyroid lobes show asymmetric uptake, and uptake also is seen along the injected vein.

In dual-isotope subtraction imaging techniques, one radiopharmaceutical (^{99m}Tc sestamibi) is used for visualization of the hyperfunctioning parathyroid gland and the thyroid gland, and a second (^{123}I or ^{99m}Tc pertechnetate) is used for visualization of the thyroid gland only. The second set of images is then digitally subtracted from the first set. Evidence of residual radioactivity on the subtraction image represents a hyperfunctioning parathyroid gland (27). Disadvantages of this subtraction method include the necessity of two radionuclide injections and of a cooperative and immobile patient, identically positioned for the two studies. In addition, there is an increased likelihood of artifacts on images obtained with digital subtraction (28,29).

The single-isotope dual-phase imaging technique was proposed on the basis of the frequently observed difference between the rate of ^{99m}Tc sestamibi washout from the thyroid gland and the rate of washout from hyperfunctioning parathyroid glands, which is typically slower (25) (Figs 4a, 4b, 5). This technique requires a single injection of ^{99m}Tc sestamibi, followed by imaging at approximately 10–15 minutes and 1.5–3 hours after the injection (27). Few studies have directly compared the subtraction technique with the double-phase technique, and their results have been conflicting (30–33). Clear superiority of one technique over the other has not been proved.

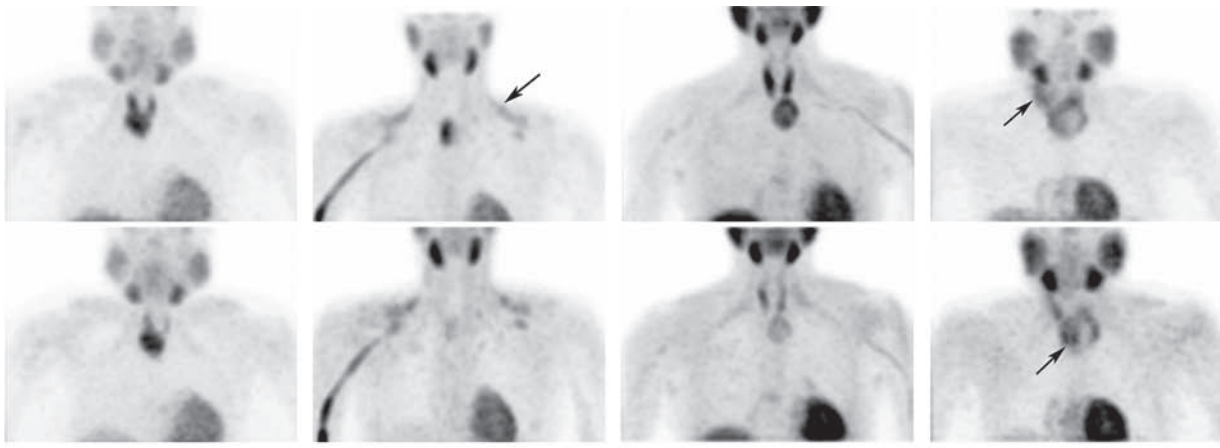

Figure 4. Anterior MIP images from early (top) and delayed (bottom) phases of SPECT in four patients with parathyroid and thyroid lesions confirmed at surgery. **(a)** Images show delayed washout in a large right inferior parathyroid adenoma that extends from the inferior pole of the right thyroid lobe to the superior mediastinum. **(b)** Images show early washout in a large right inferior parathyroid adenoma that extends to the superior mediastinum. On the early-phase image, radiotracer accumulation is visible bilaterally in the supraclavicular brown fat (arrow). **(c)** Images show early washout in a large thyroid adenoma, which extends from the lower pole of the left thyroid lobe to the superior mediastinum. No parathyroid adenomas or hyperplastic glands were identifiable on either early- or delayed-phase images; SPECT was nonlocalizing. Four-gland hyperplasia was confirmed at surgery. **(d)** Images show a papillary thyroid carcinoma, a large mass with a photopenic center and delayed heterogeneous washout that extends from the level of the left thyroid gland to the mediastinum. On the delayed-phase image (bottom), two foci of increased uptake to the left of and inferior to the mass (arrow) might be mistaken for parathyroid adenomas. The early-phase image (top) also shows an ectopic parathyroid adenoma (arrow) superior to the upper pole of the right thyroid lobe. The thyroid carcinoma and a 2.3-g parathyroid adenoma, which was located within the right carotid sheath, were surgically resected.

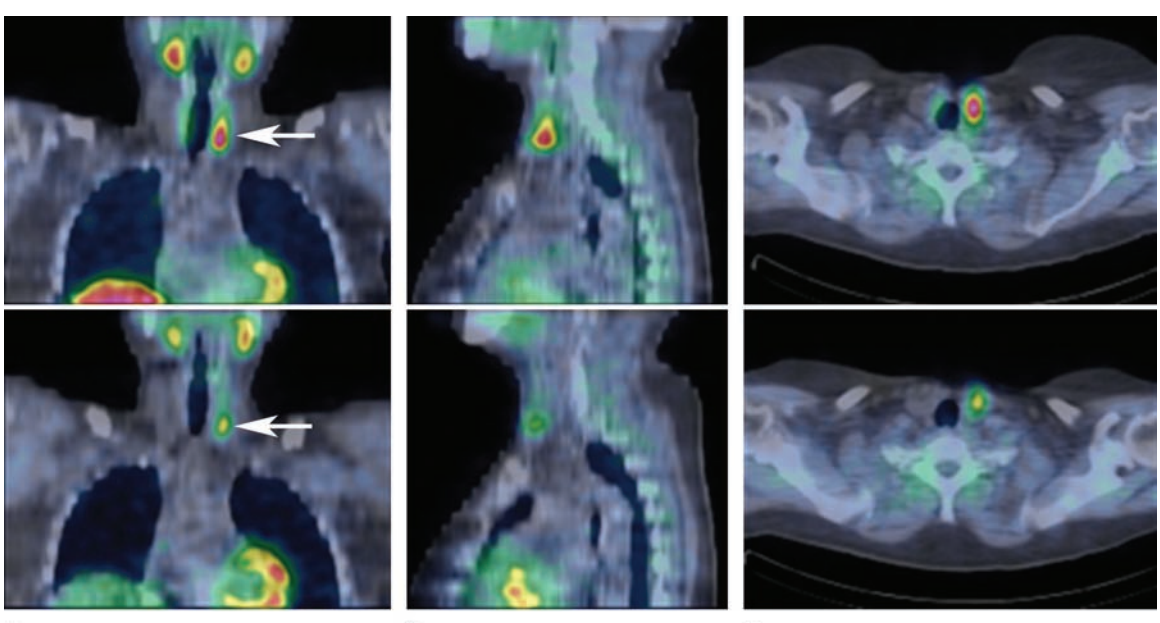

Figure 5. Eutopic left inferior parathyroid adenoma with delayed washout. Early-phase (top) and delayed-phase (bottom) coronal **(a)**, sagittal **(b)**, and axial **(c)** fused SPECT/CT images demonstrate the classic findings of a left inferior parathyroid adenoma (arrow in **a**) with a slightly anterior location at the level of the lower third of the thyroid gland.

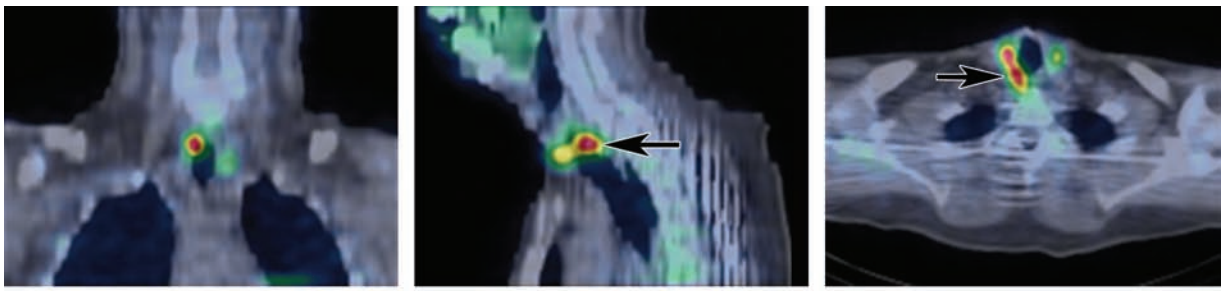

a. b. c.

Figure 6. Ectopic right superior parathyroid adenoma. Early-phase coronal **(a)**, sagittal **(b)**, and axial **(c)** fused SPECT/CT images depict typical findings of an ectopic superior parathyroid gland, with a focal area of intense ^{99m}Tc sestamibi accumulation (arrow in **b** and **c**) to the right of and posterior to the middle third of the thyroid lobe and posterolateral to the trachea.

For many years, two-dimensional planar imaging (with a parallel hole or pinhole collimator) was standard, with anterior views alone or, less commonly, combined with anterior oblique and lateral views (34,35). SPECT is used with increasing frequency today because of the three-dimensional information that it provides and because published data suggest that it has improved sensitivity for the detection and localization of hyperfunctioning parathyroid glands (36–39). The major reason for the superiority of SPECT is the improved contrast resolution (target to background). The fusion of CT images with SPECT images, either by using software (40) or by performing the studies sequentially on hybrid SPECT/CT imaging systems (14,41,42), has the advantage of combining the physiologic three-dimensional information from SPECT and anatomic information from CT; a major benefit is the more precise anatomic localization of ectopic mediastinal parathyroid adenomas (41–44). In a recent study, investigators at our institution directly compared hybrid SPECT/CT, SPECT, and planar imaging and found that early-phase SPECT/CT in combination with any delayed-phase imaging method (planar imaging, SPECT, or SPECT/CT) was statistically significantly superior to single- or dual-phase planar imaging or SPECT for parathyroid adenoma localization (14).

SPECT/CT Acquisitions

At our institution, patients receive 925–1110 MBq (25–30 mCi) of ^{99m}Tc sestamibi by intravenous injection. A hybrid SPECT/CT system (Infinia Hawkeye; GE Healthcare, Milwaukee, Wis) is used to acquire images of the neck and chest, from the level of the submandibular glands through the basal third of the heart. Two sets of images are acquired, the first at 15 minutes after injection and the second at 120 minutes.

For SPECT acquisitions, a large-field-of-view dual-detector gamma-camera system with a 20% energy window centered at 140 keV and high-resolution low-energy parallel hole collimators are used. The SPECT detectors are rotated around the patient every three degrees over a 360° arc by using a step-and-shoot protocol. One hundred twenty 25-second projection images are acquired with a matrix of 128 × 128 and a zoom factor of 1.28. Images are reconstructed by using a Butterworth prefilter (cutoff, 0.5; order, 10.0), a Butterworth postfilter (cutoff, 0.7; order, 10.0), and an ordered-subset expectation maximization iterative technique (eight subsets, two iterations). The SPECT acquisition takes approximately 25 minutes. CT image data are used for attenuation correction.

The CT data are acquired in increments of 10 mm (acquisition time, 13.84 sec per section) with a tube current of 2.5 mA and a voltage of 140 kV, and images are reconstructed to fit a matrix of 256 × 256. The CT acquisition takes approximately 10 minutes.

The reconstructed cross-sectional images are viewed on a workstation monitor (Xeleris; GE Healthcare). Maximum intensity projection (MIP) images and 3.45-mm-thick axial, coronal, and sagittal sections from SPECT and CT are displayed. The SPECT and CT images are reg-

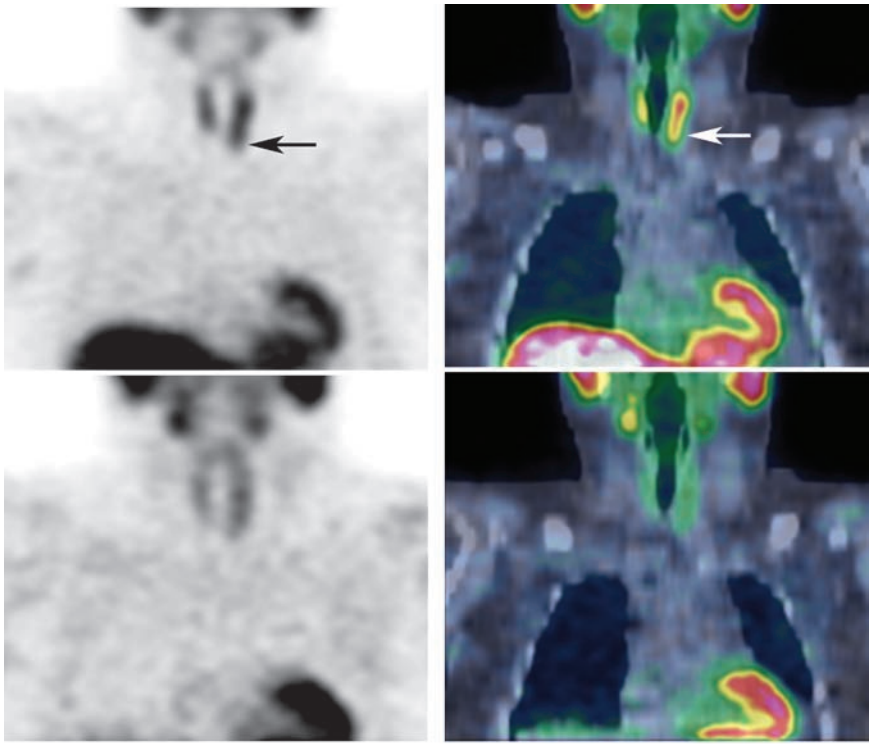

a. b.

Figure 7. Eutopic left inferior parathyroid adenoma with early washout. Early-phase (top) and delayed-phase (bottom) coronal SPECT **(a)** and fused SPECT/CT **(b)** images demonstrate an asymmetric inferior extension of the left thyroid lobe (arrow). Delayed-phase images show washout in the thyroid, with no retention of radiotracer in the region of the left inferior thyroid lobe, despite the higher intensity setting demonstrated by "hotter" salivary glands. Rapid parathyroid washout makes the diagnosis less certain, but the abnormal appearance on early-phase images is suggestive of a left inferior parathyroid adenoma, a finding that was confirmed at surgery.

istered and fused. The early- and delayed-phase SPECT raw projection images are reviewed in cinematic mode for possible patient motion. The processed images are reviewed for adequacy of the SPECT and CT image quality, attenuation correction, registration, and fusion.

SPECT/CT Image Interpretation

The primary goal of image interpretation is to detect and localize the hyperfunctioning gland or glands. In the case of parathyroid glands located at the level of the inferior part of the thyroid, the probable superior (posteriorly located) or inferior (anteriorly located) origin of the gland also should be determined.

A diagnosis of parathyroid adenoma is made by inspecting both the early-phase images and the delayed-phase images. Sometimes the diagnosis is made on the basis of findings on one or the other set of images; in other cases, it is based on combined findings from both sets of images. The early- and delayed-phase images are reviewed sequentially. Early-phase MIP images from SPECT are reviewed first; then axial, coronal, and sagittal SPECT images are registered and fused with the CT images for anatomic localization. The MIP images are particularly useful for the initial detection of parathyroid uptake or asymmetric thyroid contours that may be secondary to a parathyroid adenoma. The scintigraphic patterns observed on early-phase SPECT images depend on the relative anatomic positions and radiotracer uptake of the parathyroid and thyroid glands (45). Anatomically, the parathyroid gland may be either contiguous with or separate from the thyroid gland.

Teaching Point

On the early-phase images, a parathyroid adenoma that is separate from the thyroid may be depicted as a distinct focus of radiotracer accumulation equal to or greater than that in the thyroid (Fig 6). A parathyroid adenoma that is contiguous with the thyroid gland is detectable on early-phase images only if it has radiotracer accumulation greater than that in the thyroid gland (Fig 5) or causes an asymmetric bulging of the thyroid contour, typically of the inferior pole or posterior surface (Figs 6, 7) (46).

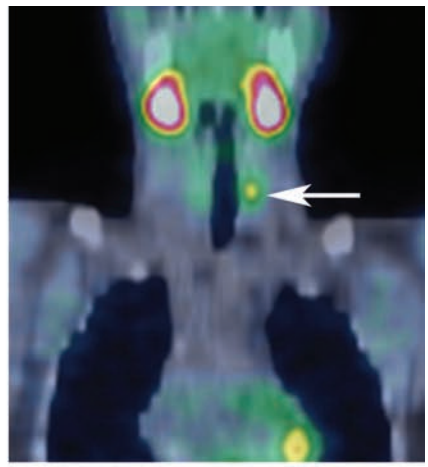

a.

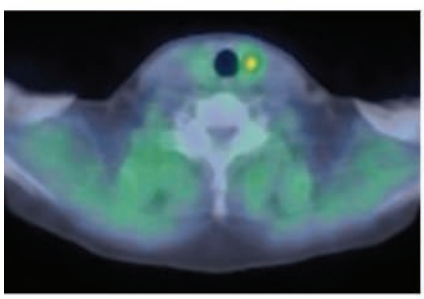

b.

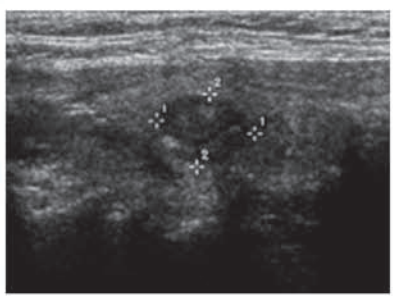

c.

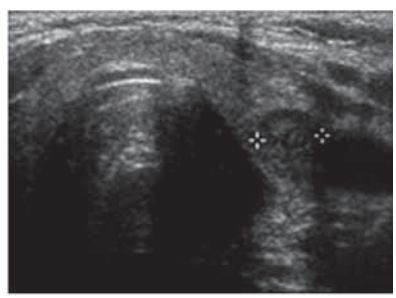

d.

Figure 8. Intrathyroidal parathyroid adenoma in an elderly woman after unsuccessful bilateral neck exploration for primary hyperparathyroidism. **(a, b)** Coronal **(a)** and axial **(b)** delayed-phase fused SPECT/CT images depict a focus of delayed washout at the level of the middle third of the left thyroid lobe (arrow in **a**). Low spatial resolution precluded differentiation of an intrathyroidal parathyroid adenoma from an adjacent extrathyroidal parathyroid adenoma. **(c, d)** Sagittal **(c)** and transverse **(d)** US images show a 12 × 9 × 8-mm hypoechoic intrathyroidal mass suggestive of a left parathyroid adenoma. The diagnosis was confirmed at surgery.

On early-phase images, intrathyroidal parathyroid adenomas that accumulate more of the radiotracer than does the thyroid gland may be detectable as asymmetric foci of increased radiotracer uptake within a thyroid lobe (Fig 8). SPECT/CT with this method usually does not allow differentiation of a parathyroid adenoma that is contiguous with the thyroid from an intrathyroidal parathyroid adenoma, because of the limited spatial resolution of SPECT and low-dose (2.5-mA) CT. However, a corresponding hypoechoic intrathyroidal mass on US images may be indicative of the diagnosis (Fig 8) (47).

Detection of a Hyperfunctioning Parathyroid Gland on Delayed-Phase Images.— Additional information may be obtained from the extent of radiotracer washout from (or differential retention in) the thyroid and parathyroid glands on delayed-phase SPECT/CT images.

Teaching Point

There are two patterns of radiotracer washout from the parathyroid glands. The more common pattern is delayed washout; early washout is less common, although not rare. Delayed washout is defined as parathyroid gland retention of the radiotracer on delayed-phase images, usually accompanied by normal washout from the thyroid (Fig 5) (25). This pattern is commonly seen in hyperfunctioning parathyroid glands, but sometimes it may be seen in the presence of a thyroid lesion (most commonly, thyroid adenoma). Early washout is defined as minimal or no retention of the radiotracer in the parathyroid gland on delayed-phase images (Fig 7) (31,39,45,48). In a series of 52 consecutive patients with primary hyperparathyroidism, delayed washout was noted in only 60% of the parathyroid adenomas (39). The differential retention of radiotracer in the hyperfunctioning parathyroid gland in comparison with that in the thyroid gland may be described as a continuum ranging from early washout (no differential retention) to delayed washout (differ-

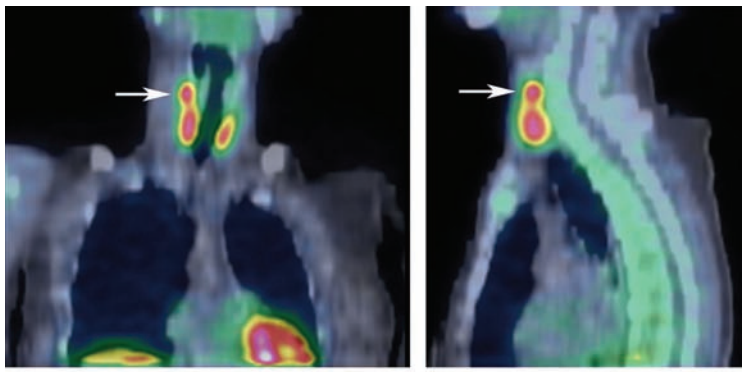

a. b.

Figure 9. Ectopic right parathyroid adenoma. Coronal **(a)** and sagittal **(b)** early-phase fused SPECT/CT images show a focus of radiotracer uptake superior to the upper pole of the right thyroid lobe (arrow). A 323-mg adenoma located medial to the right carotid artery was surgically resected.

entially increased retention in the hyperfunctioning parathyroid gland) with different degrees of relative retention in between.

There are two situations in which a delayed washout pattern provides additional diagnostic information. The first is when a parathyroid adenoma is not detected on early-phase images because it is contiguous with the thyroid gland and it accumulates a similar amount of the radiotracer, whereas delayed-phase images show a differential washout (49). The second is when an asymmetric bulging of the thyroid contour on early-phase images and delayed washout from a part of the thyroid on delayed-phase images arouses suspicion about the presence of a parathyroid adenoma.

The combination of findings that is most specific for a hyperfunctioning parathyroid gland is intense radiotracer uptake in a focal area separate from the thyroid gland on the early-phase images and delayed washout on the delayed-phase images. When the focus of intense radiotracer uptake is contiguous with the thyroid gland on early-phase images and demonstrates either delayed or early washout, a thyroid gland lesion (most commonly, thyroid adenoma) is included in the differential diagnosis (31). Knowledge of a coexistent thyroid lesion and a history of previous thyroid surgery is essential for the optimal interpretation of parathyroid functional imaging studies. Occasionally, ^{123}I or ^{99m}Tc pertechnetate scintigraphy may help define the thyroid anatomy. The pattern of radiotracer washout is neither highly specific nor highly sensitive, and it alone does not distinguish a hyperfunctioning parathyroid gland from a thyroid abnormality (Fig 4). However, any suspicious area should be reported, as such a finding may lead the surgeon to explore that area first and perform a selective parathyroidectomy rather than bilateral neck exploration. The level of interpretative certainty also should be conveyed.

Localization of Hyperfunctioning Parathyroid Glands.—SPECT/CT allows three-dimensional (lateral, supero-inferior, and anteroposterior) localization of the parathyroid glands. Lateral localization may be described as right, left, or midline (Figs 5, 6). Supero-inferior localization is best defined in relation to the thyroid gland at four levels: superior neck, thyroid gland, inferior neck, and mediastinum. The superior neck level extends downward from the angle of the mandible to the upper pole of the thyroid gland (Fig 9). The level of the thyroid gland extends from the upper pole to the lower pole and is further subdivided into three sublevels: the superior third, middle third, and inferior third of the thyroid lobes (Figs 5–7). The inferior neck level extends downward from the lower pole of the thyroid gland to the thoracic inlet. The level of the mediastinum extends downward from the thoracic inlet (Fig 10).

Anteroposterior localization of a hyperfunctioning parathyroid gland is determined in relation to the larynx, pharynx, trachea, or esophagus. Locations in the chest should be described with regard to the anterior, middle, or posterior mediastinum and other mediastinal structures (eg, great vessels, heart, and trachea) and skeletal

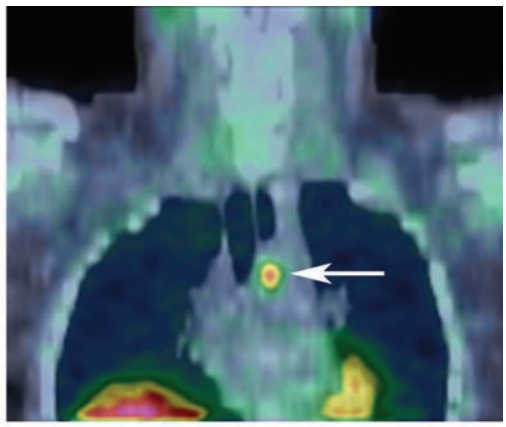

a.

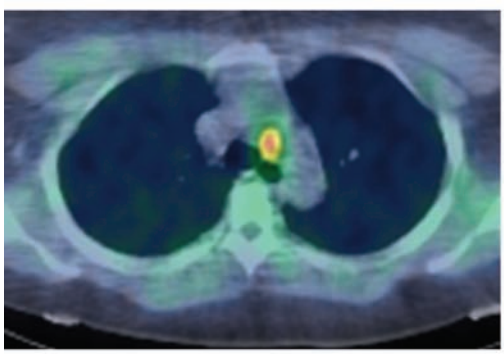

b.

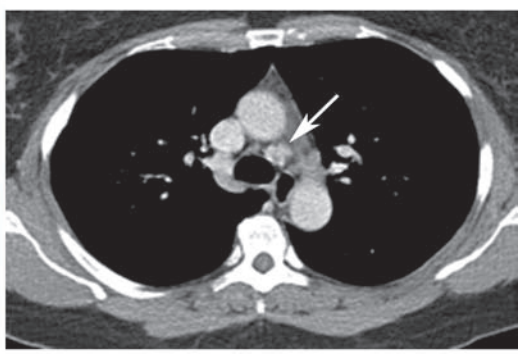

c.

Figure 10. Mediastinal parathyroid adenoma in a 52-year-old woman with persistent primary hyperparathyroidism after three-gland excision. **(a, b)** Coronal **(a)** and axial **(b)** fused early-phase SPECT/CT images depict a paratracheal mass (arrow in **a**) at the left tracheobronchial angle. **(c)** Axial CT image subsequently obtained with intravenous contrast material depicts an enhancing 12 × 13-mm left paratracheal mass (arrow) suggestive of a parathyroid adenoma. A 1.3-g adenoma was resected with a median sternotomy.

structures (manubrium, clavicle, and vertebrae). CT plays a particularly important role in the localization of ectopic mediastinal parathyroid adenomas (Fig 10). Several surgical techniques are available for accessing the anterior mediastinum (transcervical substernal approach, median sternotomy, posterolateral thoracotomy, and endoscopic dissection), and accurate localization of an ectopic mediastinal parathyroid adenoma is necessary to determine the most appropriate surgical approach (8). In cases with nonvisualization of the thyroid gland, the location of a hyperfunctioning parathyroid gland in the neck should be described by using the head of the clavicle as a landmark.

Determining the Probable Origin of a Parathyroid Gland.—Although the superior or inferior origin of a parathyroid gland often can be determined by its location, an enlarged superior parathyroid gland may migrate posteriorly and inferiorly and be seen on scintigrams at the level of the thyroid gland or inferior neck and lateral to the esophagus (paraesophageal). At the level of the inferior third of the thyroid lobe, the more posterior the location of an adenoma, the more probable that it is a descended superior parathyroid gland and not an inferior parathyroid gland (Fig 6) (8,50–53). An enlarged inferior parathyroid gland may migrate posteriorly and be detected on scintigrams at the level of the lower thyroid gland and lateral to the esophagus; in this case, the inferior origin of the parathyroid gland may be inferred from its apparent extension from the inferior pole of the thyroid gland.

Double Parathyroid Adenomas and Multiple-Gland Hyperplasia.—The same criteria apply to the detection, localization, and determination of gland origin in cases of double parathyroid adenomas (Fig 11) and multiple-gland hyperplasia. However, scintigraphy is less sensitive for multiglandular parathyroid disease (3) (Fig 4c). Therefore, if the early- and delayed-phase images do not indicate unequivocally an area suspicious for a hyperfunctioning parathyroid adenoma, the possibilities of double parathyroid

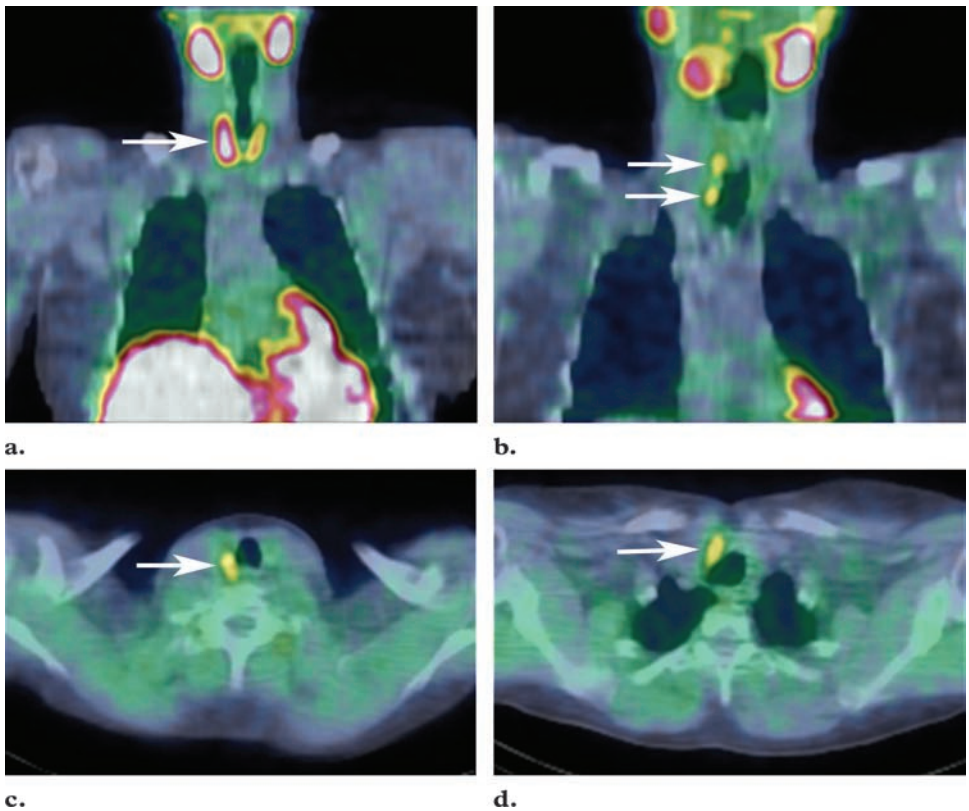

Figure 11. Double eutopic right parathyroid adenomas with delayed washout. **(a)** Coronal fused early-phase SPECT/CT image demonstrates a region in the right thyroid lobe with asymmetrically increased radiotracer uptake (arrow). **(b–d)** Coronal **(b)** and axial **(c, d)** delayed-phase fused SPECT/CT images depict two foci (arrows in **b**) with delayed washout, findings suggestive of a right superior parathyroid adenoma posterolateral to the trachea at the level of the superior third of the right thyroid lobe (arrow in **c**) and a right inferior parathyroid adenoma anterolateral to the trachea at the level of the inferior third of the thyroid lobe (arrow in **d**). A 280-mg right superior and an 820-mg right inferior parathyroid adenoma were surgically resected.

adenomas and multiple-gland hyperplasia should be considered. In a retrospective study of 401 consecutive patients with primary hyperparathyroidism, the prevalence of multiglandular disease among those with successful localization at ^{99m}Tc sestamibi scintigraphy was 4%, compared with 24% among those with unsuccessful localization (Fig 4c) (54).

Given the relative rarity of double parathyroid adenomas and multiple-gland hyperplasia (approximately 10% of cases of primary hyperparathyroidism) in comparison with coexistent thyroid abnormalities, the possibility that a second focus of uptake may be due to a thyroid lesion (eg, thyroid adenoma) should be considered. Concomitant thyroid nodules are reported with frequencies ranging from 20% to as high as 75% in endemic regions (55,56). Neck US and thyroid scintigraphy with ^{123}I or ^{99m}Tc pertechnetate may provide correlative information in these cases.

False-Positive Scintigraphic Findings

The most frequent cause of false-positive findings of a hyperfunctioning parathyroid gland at ^{99m}Tc sestamibi scintigraphy is the solid nodule that occurs in a solitary thyroid adenoma (Fig 4c) or a multinodular goiter (28). Benign or malignant tumors that take up the radiotracer and result in false-positive findings include breast, lung, and head and neck carcinomas and their lymph node and osseous metastases, as well as bronchial carcinoids (57–60). Within the neck, delayed washout of ^{99m}Tc sestamibi has been described in differentiated thyroid malignancies (Fig 4d),

primary thyroid lymphomas, a cervical lymph node metastasis from papillary thyroid carcinoma, reactive lymph nodes, a remnant thymus, a PTH-secreting paraganglioma, and an enlarged submandibular salivary gland (60–67). However, in the clinical setting of hyperparathyroidism, false-positive findings are uncommon.

False-Negative Scintigraphic Findings

Among patients with double parathyroid adenomas and four-gland hyperplasia (Fig 4c), the false-negative rate is increased, compared with that among patients with a single adenoma (3). The factor most commonly reported to correlate with false-negative findings is the size of the parathyroid gland; that is, smaller glands are less likely to be detected than larger glands. Variability of radiotracer uptake in parathyroid adenomas is another reported factor and is attributable to differences in perfusion and metabolic activity, oxyphil cell content, P-glycoprotein expression, and multidrug resistance–related protein expression and cell cycle (68–73).

Summary

Primary hyperparathyroidism is caused by a single parathyroid adenoma in up to 90% of cases. Selective surgical excision of the hyperfunctioning parathyroid gland is the treatment of choice for this condition, and parathyroid scintigraphy is the primary and standard method used for preoperative localization. SPECT is advantageous over planar imaging because it provides additional information about the anterior-posterior and superior-inferior location of parathyroid glands; CT adds further useful anatomic information. The functional and anatomic information provided by SPECT/CT makes it the preferred method for preoperative detection and localization of the cause of primary hyperparathyroidism.

References

1. Kearns AE, Thompson GB. Medical and surgical management of hyperparathyroidism. Mayo Clin Proc 2002;77(1):87–91. [Published correction appears in Mayo Clin Proc 2002;77(3):298.]
2. Taniegra ED. Hyperparathyroidism. Am Fam Physician 2004;69(2):333–339.
3. Ruda JM, Hollenbeak C, Stack BC Jr. A systematic review of the diagnosis and treatment of primary hyperparathyroidism from 1995 to 2003. Otolaryngol Head Neck Surg 2005;132(3):359–372.
4. Russell CF, Laird JD, Ferguson WR. Scan-directed unilateral cervical exploration for parathyroid adenoma: a legitimate approach? World J Surg 1990; 14(3):406–409.
5. Suliburk JW, Perrier ND. Primary hyperparathyroidism. Oncologist 2007;12(6):644–653.
6. Harnsberger HR, Osborn AG, Ross J, Macdonald A. Thyroid gland and parathyroid glands. In: Diagnostic and surgical imaging anatomy: brain, head and neck, spine. Salt Lake City, Utah: Amirsys, 2006.
7. Dufour DR, Wilkerson SY. Factors related to parathyroid weight in normal persons. Arch Pathol Lab Med 1983;107(4):167–172.
8. Pellitteri PK, Sofferman RA, Randolph GW. Surgical management of parathyroid disorders. In: Cummings CW, Haughey BH, Thomas JR, Harker LA, Flint PW, eds. Cummings otolaryngology: head and neck surgery. 4th ed. Philadelphia, Pa: Mosby, 2005.
9. Phitayakorn R, McHenry CR. Incidence and location of ectopic abnormal parathyroid glands. Am J Surg 2006;191(3):418–423.
10. DeLellis RA. Surgical pathology of the parathyroid glands. In: Randolph G, ed. Surgery of the thyroid and parathyroid glands. St. Louis, Mo: Elsevier, 2003;571–577.
11. Bilezikian JP, Silverberg SJ. Clinical practice. Asymptomatic primary hyperparathyroidism. N Engl J Med 2004;350(17):1746–1751.
12. Bilezikian JP, Potts JT Jr, Fuleihan Gel-H, et al. Summary statement from a workshop on asymptomatic primary hyperparathyroidism: a perspective for the 21st century. J Clin Endocrinol Metab 2002;87(12):5353–5361.
13. Rubello D, Giannini S, De Carlo E, et al. Minimally invasive (99m)Tc-sestamibi radioguided surgery of parathyroid adenomas. Panminerva Med 2005;47(2):99–107.
14. Lavely WC, Goetze S, Friedman KP, et al. Comparison of SPECT/CT, SPECT, and planar imaging with single- and dual-phase 99mTc-sestamibi parathyroid scintigraphy. J Nucl Med 2007;48(7): 1084–1089.
15. Rodgers SE, Hunter GJ, Hamberg LM, et al. Improved preoperative planning for directed parathyroidectomy with 4-dimensional computed tomography. Surgery 2006;140(6):932–940.
16. Lumachi F, Zucchetta P, Marzola MC, et al. Advantages of combined technetium-99m-sestamibi scintigraphy and high-resolution ultrasonography in parathyroid localization: comparative study in 91 patients with primary hyperparathyroidism. Eur J Endocrinol 2000;143(6):755–760.
17. Solorzano CC, Carneiro-Pla DM, Irvin GL 3rd. Surgeon-performed ultrasonography as the initial and only localizing study in sporadic and primary hyperparathyroidism. J Am Coll Surg 2006;202(1): 18–24.
18. Ahuja AT, Wonga KT, Ching AS, et al. Imaging for primary hyperparathyroidism—what beginners should know. Clin Radiol 2004;59(11):967–976.
19. Johnson NA, Tublin ME, Ogilvie JB. Parathyroid imaging: technique and role in the preoperative evaluation of primary hyperparathyroidism. AJR Am J Roentgenol 2007;188(6):1706–1715.

20. Ferlin G, Borsato N, Camerani M, Conte N, Zotti D. New perspectives in localizing enlarged parathyroids by technetium-thallium subtraction scan. J Nucl Med 1983;24(5):438–441.
21. Coakley AJ, Kettle AG, Wells CP, O'Doherty MJ, Collins RE. 99mTc-sestamibi—a new agent for parathyroid imaging. Nucl Med Commun 1989; 10(11):791–794.
22. Bergenfelz A, Tennvall J, Valdermarsson S, Lindblom P, Tibblin S. Sestamibi versus thallium subtraction scintigraphy in parathyroid localization: a prospective comparative study in patients with predominantly mild primary hyperparathyroidism. Surgery 1997;121(6):601–605.
23. Casas AT, Burke GJ, Sathyanarayana, Mansberger AR Jr, Wei JP. Prospective comparison of technetium-99m-sestamibi/iodine-123 radionuclide scan versus high-resolution ultrasonography for the preoperative localization of abnormal parathyroid glands in patients with previously unoperated primary hyperparathyroidism. Am J Surg 1993; 166(4):369–373.
24. Weber CJ, Vansant J, Alazraki N. Value of technetium-99m-sestamibi iodine-123 imaging in reoperative parathyroid surgery. Surgery 1993;114(6): 1011–1018.
25. Taillefer R, Boucher Y, Potvin C, Lambert R. Detection and localization of parathyroid adenomas in patients with hyperparathyroidism using a single radionuclide imaging procedure with technetium-99m-sestamibi (double-phase study). J Nucl Med 1992;33(10):1801–1807.
26. Arbab AS, Koizumi K, Toyama K, Araki T. Uptake of technetium-99m-tetrofosmin, technetium-99m-MIBI and thallium-201 in tumor cell lines. J Nucl Med 1996;37(9):1551–1556.
27. Palestro CJ, Tomas MB, Tronco GG. Radionuclide imaging of the parathyroid glands. Semin Nucl Med 2005;35(4):266–276.
28. Sandrock D, Merino MJ, Norton JA, Neumann RD. Parathyroid imaging by Tc/Tl scintigraphy. Eur J Nucl Med 1990;16(8–10):607–613.
29. Liehn JC, Delisle MJ, Flament JB. Improvement of parathyroid Tl-Tc scintigraphy by using a new image subtraction method. Eur J Nucl Med 1988; 14(4):184–189.
30. Rauth JD, Sessions RB, Shupe SC, Ziessman HA. Comparison of Tc-99m MIBI and Tl-201/Tc-99m pertechnetate for diagnosis of primary hyperparathyroidism. Clin Nucl Med 1996;21(8):602–608.
31. Chen CC, Holder LE, Scovill WA, Tehan AM, Gann DS. Comparison of parathyroid imaging with technetium-99m-pertechnetate/sestamibi subtraction, double-phase technetium-99m-sestamibi and technetium-99m-sestamibi SPECT. J Nucl Med 1997;38(6):834–839.
32. Neumann DR, Esselstyn CB Jr, Go RT, Wong CO, Rice TW, Obuchowski NA. Comparison of double-phase 99mTc-sestamibi with 123I-99mTc-sestamibi subtraction SPECT in hyperparathyroidism. AJR Am J Roentgenol 1997;169(6):1671–1674.
33. Leslie WD, Dupont JO, Bybel B, Riese KT. Parathyroid 99mTc-sestamibi scintigraphy: dual-tracer subtraction is superior to double-phase washout. Eur J Nucl Med Mol Imaging 2002;29(12): 1566–1570.
34. Krausz Y, Horne T, Wynchank S, Halevy A. Lateral neck imaging for spatial localization of parathyroid tissue. Nucl Med Biol 1995;22(3):391–394.
35. Arveschoug AK, Bertelsen H, Vammen B, Brochner-Mortensen J. Preoperative dual-phase parathyroid imaging with tc-99m-sestamibi: accuracy and reproducibility of the pinhole collimator with and without oblique images. Clin Nucl Med 2007; 32(1):9–12.
36. Moka D, Voth E, Dietlein M, Larena-Avellaneda A, Schicha H. Technetium 99m-MIBI-SPECT: a highly sensitive diagnostic tool for localization of parathyroid adenomas. Surgery 2000;128(1): 29–35.
37. Schachter PP, Issa N, Shimonov M, Czerniak A, Lorberboym M. Early, postinjection MIBI-SPECT as the only preoperative localizing study for minimally invasive parathyroidectomy. Arch Surg 2004; 139(4):433–437.
38. Slater A, Gleeson FV. Increased sensitivity and confidence of SPECT over planar imaging in dual-phase sestamibi for parathyroid adenoma detection. Clin Nucl Med 2005;30(1):1–3.
39. Lorberboym M, Minski I, Macadziob S, Nikolov G, Schachter P. Incremental diagnostic value of preoperative 99mTc-MIBI SPECT in patients with a parathyroid adenoma. J Nucl Med 2003;44(6): 904–908.
40. Profanter C, Wetscher GJ, Gabriel M, et al. CT-MIBI image fusion: a new preoperative localization technique for primary, recurrent, and persistent hyperparathyroidism. Surgery 2004;135(2):157–162.
41. Gayed IW, Kim EE, Broussard WF, et al. The value of 99m-Tc-sestamibi SPECT/CT over conventional SPECT in the evaluation of parathyroid adenomas and hyperplasia. J Nucl Med 2005;46(2): 248–252.
42. Krausz Y, Bettman L, Guralnik L, et al. Technetium-99m-MIBI SPECT/CT in primary hyperparathyroidism. World J Surg 2006;30(1):76–83.
43. Kaczirek K, Prager G, Kienast O, et al. Combined transmission and (99m)Tc-sestamibi emission tomography for localization of mediastinal parathyroid glands. Nuklearmedizin 2003;42(5):220–223.
44. Ruf J, Seehofer D, Denecke T, et al. Impact of image fusion and attenuation correction by SPECT-CT on the scintigraphic detection of parathyroid adenomas. Nuklearmedizin 2007;46(1):15–21.
45. Chen CC, Skarulis MC, Fraker DL, Alexander R, Marx SJ, Spiegel AM. Technetium-99m-sestamibi imaging before reoperation for primary hyperparathyroidism. J Nucl Med 1995;36(12):2186–2191.
46. Bajoghli M, Muthukrishnan A, Mountz J. Posterior bulge sign for parathyroid adenoma on Tc-99m MIBI SPECT. Clin Nucl Med 2006;31(8): 470–471.
47. Yusim A, Aspelund G, Ahrens W, et al. Intrathyroidal parathyroid adenoma. Thyroid 2006;16(6): 619–620.
48. Benard F, Lefebvre B, Beuvon F, Langlois MF, Bisson G. Rapid washout of technetium-99m-MIBI from a large parathyroid adenoma. J Nucl Med 1995;36(2):241–243.

49. Sfakianakis GN, Irvin GL 3rd, Foss J, et al. Efficient parathyroidectomy guided by SPECT-MIBI and hormonal measurements. J Nucl Med 1996; 37(5):798–804.
50. Chan TY, Serpell JW, Chan O, Gaunt JI, Young AE, Nunan TO. Misinterpretation of the upper parathyroid adenoma on thallium-201/technetium-99m subtraction scintigraphy. Br J Radiol 1991; 64(757):1–4.
51. Kim SC, Kim S, Inabet W, Krynyckyi B, Machec J, Kim CK. Appearance of descended superior parathyroid adenoma on SPECT parathyroid imaging. Clin Nucl Med 2007;32(2):90–93.
52. Taieb D, Hassad R, Sebag F, et al. Tomoscintigraphy improves the determination of the embryologic origin of parathyroid adenomas, especially in apparently inferior glands: imaging features and surgical implications. J Nucl Med Technol 2007;35(3): 135–139.
53. Clark PB, Case D, Watson NE Jr, Perrier ND, Morton KA. Enhanced scintigraphic protocol required for optimal preoperative localization before targeted minimally invasive parathyroidectomy. Clin Nucl Med 2003;28(12):955–960.
54. Chiu B, Sturgeon C, Angelos P. What is the link between nonlocalizing sestamibi scans, multigland disease, and persistent hypercalcemia? A study of 401 consecutive patients undergoing parathyroidectomy. Surgery 2006;140(3):418–422.
55. Lumachi F, Marzola MC, Zucchetta P, Tregnaghi A, Cecchin D, Bui F. Hyperfunctioning parathyroid tumours in patients with thyroid nodules: sensitivity and positive predictive value of high-resolution ultrasonography and 99mTc-sestamibi scintigraphy. Endocr Relat Cancer 2003;10(3):419–423.
56. Erbil Y, Barbaros U, Yanik BT, et al. Impact of gland morphology and concomitant thyroid nodules on preoperative localization of parathyroid adenomas. Laryngoscope 2006;116(4):580–585.
57. Taillefer R, Robidoux A, Lambert R, Turpin S, Laperriere J. Technetium-99m-sestamibi prone scintimammography to detect primary breast cancer and axillary lymph node involvement. J Nucl Med 1995;36(10):1758–1765.
58. Yen TC, Tzen KY, Lee CM, Tsai CC. Squamous cell carcinoma of the lung mimicking an ectopic mediastinal parathyroid adenoma demonstrated by Tc-99m sestamibi in a hypercalcemic patient. Clin Nucl Med 1999;24(11):895–896.
59. Yapar Z, Kibar M, Sukan A, Paydas S, Zeren H, Inal M. Coincidental visualization of an atypical bronchial carcinoid on Tc-99m-sestamibi scan in Kallmann's syndrome. Ann Nucl Med 2002;16(1): 61–65.
60. Glaser C, Pruckmayer M, Staudenherz A, Rasse M, Lang S, Leitha T. Utility of technetium-99m-sestamibi to assess osseous tumour spread. J Nucl Med 1996;37(9):1526–1528.
61. Koss WG, Brown MR, Balfour JF. A false-positive localization of a parathyroid adenoma with technetium Tc 99m sestamibi scan secondary to a thyroid follicular carcinoma. Arch Surg 1996;131(2): 216–217.
62. Scott AM, Kostakoglu L, O'Brien JP, Straus DJ, Abdel-Dayem HM, Larson SM. Comparison of technetium-99m-MIBI and thallium-201-chloride uptake in primary thyroid lymphoma. J Nucl Med 1992;33(7):1396–1398.
63. Shanmugam N, Johns W, Chasse K, Gupta SM. Serendipitous detection of metastatic thyroid cancer during I-123 Tc-99m sestamibi dual parathyroid imaging. Clin Nucl Med 2005;30(8):550–551.
64. Leslie WD, Riese KT, Mohamed C. Sestamibi retention in reactive lymph node hyperplasia: a cause of false-positive parathyroid localization. Clin Nucl Med 2000;25(3):216–217.
65. Mudun A, Kocak M, Unal S, Cantez S. Tc99m MIBI accumulation in remnant thymus: a cause of false-positive interpretation in parathyroid imaging. Clin Nucl Med 1995;20(4):379–380.
66. Bhattacharya A, Mittal BR, Bhansali A, Radotra BD, Behera A. Cervical paraganglioma mimicking a parathyroid adenoma on Tc-99m sestamibi scintigraphy. Clin Nucl Med 2006;31(4):234–236.
67. Campeau RJ, Reuther WL, Wayne J. False-positive Tc99m sestamibi examination for parathyroid adenoma in a case of asymmetrical salivary gland enlargement. Clin Nucl Med 1999;24(9):723–724.
68. Bhatnagar A, Vezza PR, Bryan JA, Atkins FB, Ziessman HA. Technetium-99m-sestamibi parathyroid scintigraphy: effect of P-glycoprotein, histology and tumor size on detectability. J Nucl Med 1998;39(9):1617–1620.
69. Torregrosa JV, Fernandez-Cruz L, Canalejo A, et al. 99mTc-sestamibi scintigraphy and cell cycle in parathyroid glands of secondary hyperparathyroidism. World J Surg 2000;24(11):1386–1390.
70. Sun SS, Shiau YC, Lin CC, Kao A, Lee CC. Correlation between P-glycoprotein (P-gp) expression in parathyroid and Tc-99m MIBI parathyroid image findings. Nucl Med Biol 2001;28(8):929–933.
71. Pons F, Torregrosa JV, Fuster D. Biological factors influencing parathyroid localization. Nucl Med Commun 2003;24(2):121–124.
72. Pinero A, Rodriguez JM, Martinez-Barba E, Canteras M, Stiges-Serra A, Parrilla P. Tc99m-sestamibi scintigraphy and cell proliferation in primary hyperparathyroidism: a causal or casual relationship? Surgery 2003;134(1):41–44.
73. Turgut B, Elagoz S, Erselcan T, et al. Preoperative localization of parathyroid adenomas with technetium-99m methoxyisobutylisonitrile imaging: relationship with P-glycoprotein expression, oxyphilic cell content, and tumoral tissue volume. Cancer Biother Radiopharm 2006;21(6):579–590.

This article meets the criteria for 1.0 credit hour in category 1 of the AMA Physician's Recognition Award. To obtain credit, see accompanying test at http://www.rsna.org/education/rg_cme.html.

RadioGraphics

Parathyroid Scintigraphy in Patients with Primary Hyperparathyroidism: ^{99m}Tc Sestamibi SPECT and SPECT/CT

Hedieh K. Eslamy and Harvey A. Ziessman

RadioGraphics 2008; 28:1461–1476 • **Published online** 10.1148/rg.285075055 • **Content Codes:** CT HN NM

Page 1463
Eutopic superior parathyroid glands are posterior to the superior or middle third of the thyroid lobe; eutopic inferior parathyroid glands are anterior, lateral, or posterior to the inferior third of the thyroid lobe.

Page 1464
Primary hyperparathyroidism may be sporadic or familial. The cause in most cases is a single parathyroid adenoma (90% of cases); less common causes include double adenomas (4%), hyperplasia of multiple glands (6%), and parathyroid carcinoma (<1%).

Page 1466
Three general techniques of radionuclide scintigraphy are commonly used for the detection and visualization of hyperfunctioning parathyroid glands: single-phase dual-isotope subtraction imaging, dual-phase single-isotope imaging, and a combination of the two.

Page 1469
The scintigraphic patterns observed on early-phase SPECT images depend on the relative anatomic positions and radiotracer uptake of the parathyroid and thyroid glands.

Page 1470
There are two patterns of radiotracer washout from the parathyroid glands. The more common pattern is delayed washout; early washout is less common, although not rare.